source; $\overline{\sigma}$ and $\overline{M}$, coefficients in the linear approximation for the electrical conductivity and density; R, active resistance of the chain; v, velocity. Indices: 0, equilibrium state of the arc; a, arc; ℓ, differentiation with respect to the velocity v_0; an overdot indicates a time derivative.

LITERATURE CITED

1. G. Mekker, TIIÉR, 59, No. 4, 4-14 (1971).
2. D. E. Anderson, Transport Phenomena in Thermal Plasma [Russian translation], Moscow (1972).
3. P. A. Kulakov, Thermophysics and Physical Hydrodynamics [in Russian], Novosibirsk (1978), pp. 126-134.
4. A. A. Andronov, A. A. Vitt, and S. É. Khaikin, Theory of Oscillations [in Russian], Moscow (1981).
5. V. D. Khait, Teplofiz. Vys. Temp., 18, No. 3, 489-496 (1980).
6. V. I. Artemov, I. N. Rutkevich, and O. A. Sinkevich, Teplofiz. Vys. Temp., 18, No. 6, 1126-1136 (1980).
7. M. F. Zhukov, A. S. Koroteev, and B. A. Uryukov, Applied Dynamics of Thermal Plasma [in Russian], Novosibirsk (1975).
8. M. F. Zhukov (ed.), Theory of Electric Arc Under Conditions of Forced Heat Exchange [in Russian], Novosibirsk (1977).
9. O. Ya. Novikov, Stability of an Electric Arc [in Russian], Leningrad (1978).
10. N. V. Pashatskii and S. G. Lisitsyn, Inzh.-Fiz. Zh., 47, 133-139 (1984).

COMPUTATION OF THE DYNAMICS OF SWIRLING VORTEX FLOW IN A CYLINDER OF AN INTERNAL-COMBUSTION ENGINE DURING THE COMPRESSION STROKE

M. A. Gorokhovskii and V. P. Khlynin

UDC 517.944:532.525.6

The vortex flow configuration in an engine cylinder is calculated for various geometries of an undivided combustion chamber. The data of a numerical analysis and experimental measurements are compared.

1. Three types of internal-combustion (IC) engine models are known in the literature [1-3]. The first type refers to thermodynamic or zero-dimensional models [4], whose parameters (velocity, temperature, concentration, pressure, etc.) are averaged over the volume of the combustion chamber and are functions of only one variable: time [5-8]. The analyzed region of the combustion chamber is partitioned into the zones of the fresh charge and the combustion products; the partition of each of them is described by thermodynamic relations formulated on the basis of the ideal-gas energy balance equations and equations of state. Thermodynamic models are concerned primarily with the analysis of turbulent mixing rates and the influence of turbulence on the flame propagation velocity. Combustion is treated here as the propagation of a laminar flame front of finite width via discrete turbulent vortices. An elaboration of this approach may be found in [8], where the mixing and combustion processes are described (with allowance for semiempirical information on the individual structure of the vortices) by statistical modeling.

In quasidimensional models [9, 10], the machinery developed in thermodynamic models is augmented with a semiempirical theory of the propagation of a one-dimensional turbulent flame.

The simplifications associated with the formulation of zero-dimensional and quasidimensional models are significantly manifested in the modeling of stratified-charge fuel-injection engines and in diesel engines, where the rate of heat release through chemical reactions is primarily mixing-controlled. Detailed engine models have been proposed in a number of papers [11-19] in order to describe the mixing processes with allowance for the contri-

S. M. Kirov Kazakh State University, Alma-Ata.

Translated from Inzhenerno-Fizicheskii Zhurnal, Vol. 51, No. 4, pp. 654-660, October, 1986. Original article submitted June 20, 1985.

0022-0841/86/5104-1238$12.50

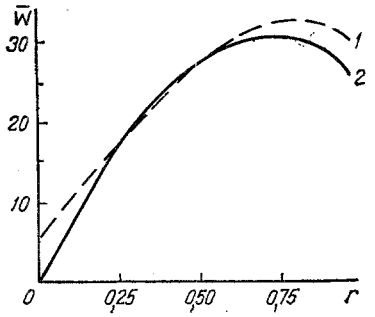

Fig. 1. Comparison of the computed and experimental [35] distributions of the azimuthal velocity $\bar{W}$ (m/sec). 1) Experimental; 2) computed.

bution of wall effects, flow rotation (swirling), and the combustion chamber geometry. In this case it is necessary to perform numerical integration of time-dependent partial differential equations "controlled" by turbulent heat and mass transfer in multicomponent mixtures with chemical conversions and a moving boundary. Although the flow pattern in real engines, as a rule, is fully three-dimensional, the two-dimensional mathematical formulation of the detailed models, which is used by virtue of limitations of computer resources, preserves the general trends and properties of the investigated physical situations. In particular, the flow near top dead center (TDC) has been investigated in the plane normal to the axis of the cylinder within the framework of the two-dimensional representation [20-22]. Schock et al. [23, 24] have used a cylindrical coordinate system, in which the swirling flow of the gas mixture has axial symmetry. Both of these two-dimensional formulations complement one another, and the choice of a particular two-dimensional description is dictated by practical engineering requirements.

2. In the present study, to illustrate the effectiveness of the detailed models, we carry out systematic computations of the turbulent gas dynamics of a diesel engine with an undivided combustion chamber in the compression stroke. We discuss the influence of the chamber geometry on the spatial configuration of the vortex flow in the IC engine cylinder. We also compare the experimental profile of the swirling velocity with the numerical analysis data.

3. We assume that the values of the pressure, density, velocity, temperature, etc., can be regarded as identical in a plane normal to the cylinder axis around any circle concentric with this axis. Accordingly, we write the heat- and mass-transfer equations in cylindrical coordinates (R, Z, ε) with axial symmetry and a nonzero azimuthal velocity. They appear as follows in vector notation.

Momentum transfer equation:

$$\frac{\partial}{\partial t}(\rho\mathbf{V})+\frac{1}{R}\nabla\cdot(R\rho\mathbf{V}\cdot\mathbf{V})=-\nabla P+\frac{1}{R}\nabla\cdot(R\tilde{\sigma})-\frac{\sigma_0-\rho W^2}{R}\mathbf{r}, \tag{1}$$

where $\sigma_0 = 2\mu(\mathbf{V}\cdot\mathbf{r}) - 2/3\ \mu\nabla\cdot\mathrm{RV}$. We write the stress tensor everywhere, according to the generalized Newton's law, in the form

$$\tilde{\sigma}=2\mu\,\mathrm{def}\,\mathbf{V}-\frac{2}{3}\mu(\nabla\cdot R\mathbf{V})\tilde{\varepsilon},$$

where $\tilde{\varepsilon}$ is the unit tensor and the components of the tensor $(\mathrm{def}\ \mathrm{V})_{ij} = \frac{1}{2}\left(\frac{\partial V_i}{\partial x_j}+\frac{\partial V_j}{\partial x_i}\right)$ are evaluated in cylindrical coordinates.

Equation for the azimuthal velocity W:

$$\frac{\partial}{\partial t}(\rho RW)+\frac{1}{R}\nabla\cdot(\rho R^2W\mathbf{V})=\frac{1}{R}\nabla\cdot(R\tau), \tag{2}$$

where $\tau = R^2\nabla(W/R)$.

Equation for the mass fractions of the components of the mixture:

$$\frac{\partial Y_k}{\partial t}+\frac{1}{R}\nabla\cdot(RY_k\mathbf{V})=\frac{1}{R}\nabla\cdot(R\rho D\nabla Y_k). \tag{3}$$

The sum of the mass fractions in the mixture must be equal to unity:

$$\sum_k Y_k=1. \tag{4}$$

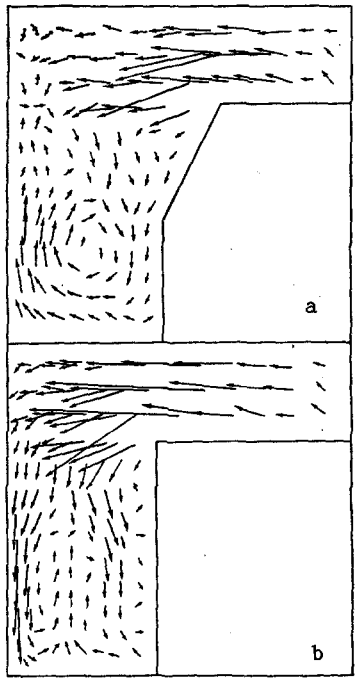

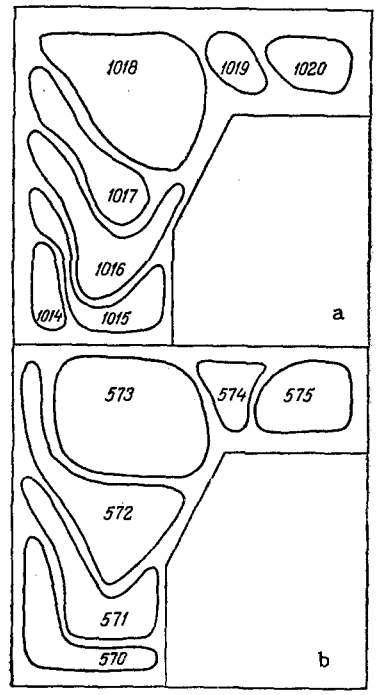

Fig. 2 Fig. 3

Fig. 2. Flow configuration for various piston surface geometries at $\alpha = 170°$ from BDC.

Fig. 3. Distribution of the isotherms at $\alpha = 170°$ from BDC. a) $T_0 = 433°K$; b) 230°K.

When Eq. (3) is summed over k, the equation of continuity takes the following form with allowance for (4):

$$\frac{\partial \rho}{\partial t} + \frac{1}{R} \nabla \cdot (R\rho \mathbf{V}) = 0. \tag{5}$$

The internal-energy (I) balance equation has the form

$$\frac{\partial}{\partial t}(\rho I) + \frac{1}{R} \nabla \cdot (R\rho I \mathbf{V}) = -\frac{P}{R} \nabla \cdot (R\mathbf{V}) + \tilde{\sigma} : \mathrm{Grad}\, \mathbf{V} + \tau \cdot \nabla \frac{W}{R} + \frac{\sigma_0}{R} \mathbf{V} \cdot \mathbf{r} - \frac{1}{R} \nabla \cdot (R\mathbf{J}), \tag{6}$$

where J is the diffusion heat flux, which is determined by thermal conduction and energy transport effects due to interdiffusion of the mixture components:

$$J = -\lambda \nabla T - \rho D \sum_k h_k \nabla Y_k, \tag{7}$$

and the quantities λ and D are determined in terms of the Prandtl and Schmidt numbers and the effective viscosity: $\lambda = \mu C_V / \mathrm{Pr}$; $D = \mu/(\rho \mathrm{Sc})$. The mathematical formulation is augmented with the ideal-gas thermodynamic relations for the mixture:

$$P = R_1 T \rho \sum_k \frac{Y_k}{\omega_k}; \tag{8}$$

$$I(T) = \sum_k Y_k I_k(T); \tag{9}$$

$$C_v(T) = \sum_k Y_k C_{vk}(T); \tag{10}$$

$$h_k = I_k + \frac{R_1 T}{\omega_k}. \tag{11}$$

The values of the function $I_k(T)$ are tabulated in [25]. These tables are used to find the temperature by a linear search algorithm with allowance for the fact that the derivative $\partial I/\partial T$ is always positive.

These equations have been formulated for laminar flows. However, if each individual variable is represented by the sum of a mean (e.g., the Favre mean) component and a pulsation component and if the turbulent diffusion is modeled by gradient-type relations, turbulent flows can be described on the basis of the same equations.

4. We assume that the spectral function of the turbulent energy depends on the energy input rate (on the distribution of the mean-velocity deformation field) for turbulence space scales commensurate with the geometrical scales of the flow and greater than the control mesh size of the differencing grid. The form of the turbulent energy spectral function for turbulence scales smaller than the control mesh size is considered to be universal and to obey the laws of the inertial interval of wave numbers. The spectrum of the small-scale components and their energy "supply" from large energy-transporting vortices play a decisive role in the "subgrid" modeling problem [26, 27]. However, the detailed analysis of the dynamics of small-scale vortices is prohibited by computer power limitations. Here, in accordance with [28, 29], we represent the influence of these vortices by means of the vortex viscosity, the expression for which contains a turbulence scale equal to the control mesh size of the computing grid:

$$\nu = \frac{\mu}{\rho} = (C\Delta)^2 \cdot [(\mathrm{def}\,\mathbf{V})_{ij}\,(\mathrm{def}\,\mathbf{V})_{ij}]^{1/2}, \tag{12}$$

where C = 0.2 and i, j = 1, 2, 3 are the summation indices. It has been shown [30] that this kind of operation of artificially enlarging the dissipative turbulence microscale to the mesh sizes of the differencing grid is analogous to the introduction of the Neumann–Richtmyer artificial viscosity for shock waves. The effective viscosity coefficient is determined from the relation $\mu = \mu_T + \mu_L$, where μ_L obeys Sazerlend's law.

The law of the wall, which permits the surface frictional stress to be determined, is used for spatial resolution of the thin turbulent boundary layer at the wall of the cylinder. The values of the velocity and temperature on the surface of the cylinder are specified according to the no-slip and adiabaticity conditions (or specification of a constant temperature), respectively.

5. The algorithm developed in [14, 2, 24] for the numerical integration of Eqs. (1)-(11) is based on the fundamental principles of the ECE explicit-implicit method [31, 32] for the evolving spatial differences of rectangular cells of arbitrary form, whose nodes move together with the gas and thus automatically adjust the grid geometry to the nature of the gasdynamic flow (ALE method [33, 34]). The time-splitting procedure in the combined ICE–ALE method comprises three phases. The first phase entails an explicit Lagrange computation of the hydrodynamic and thermodynamic parameters of the flow. It is assumed here that the nodes of the mesh cells move with the velocity of the medium in such a way that the convection terms in the transport equations vanish. The distributions of the partial and total masses in the cells are computed, along with the coordinates of the nodes, the profiles of the velocity components, the internal energy, the temperature, and the pressure. The second phase of the procedure entails the formulation of an iterative procedure for refining the velocity, internal-energy, and pressure fields in such a way so that the grid sources of mass, momentum, and energy will tend to zero. In the third phase, the grid distributions of the individual variables are recomputed with allowance for the transfer associated with motion of the medium relative to the moving grid.

6. Figure 1 shows the results of a comparison of the computed azimuthal velocity (W) profile with the measured [35] distribution for an engine operating at 1200 rpm, at 370° from TDC, and for a flat piston surface. The initial temperature of the compressed air is specified to be identical at all points and equal to 373°K. The nonzero value of the swirl velocity at the cylinder axis can be attributed to precession, which takes place in three-dimensional flows. The initial distributions of all the parameters of the air are specified at 315° from TDC. The data at 310° and 320° from TDC are averaged in order to have some way of taking precession effects into account in the specification of the initial radial distribution of the azimuthal velocity at 315° from TDC. The initial distributions for the radial and axial components of the velocity are evaluated according to the conditions of uniform axial compression of the air. The isothermal surface of the cylinder is maintained at a temperature of 300°K. It is evident, even for such a simplified mathematical description of the problem (the "coarse" turbulence model, the two-dimensional formulation, and unrealistic initial conditions), that the agreement of the numerical and experimental values of the azimuthal velocity of rotation of the air flow is quite good.

Figure 2 shows the flow configuration of a mixture of nitrogen, oxygen, and carbon dioxide at 170° from bottom dead center (BDC) for various piston surface geometries in diesel engines with an undivided combustion chamber. The figure shows the velocity distributions of the gas mixture just before fuel injection; they characterize the flow pattern prior to mixing of the fuel with the oxidizing agent. It is evident from this figure, that a variation of the piston surface geometry affects the flow structure of the mixture, in particular, the formation of large vortices and their direction of rotation in the combustion chamber.

The existence of an almost uniform temperature distribution (at $\alpha = 170°$ from BDC) in the compression process is evinced by the isotherms in Fig. 3, which are shown for various values of the initial temperature of the gas mixture. The expression for estimation of the temperature of the mixture in the compression stroke is satisfied quite accurately $T = 2.5T_0$.

NOTATION

R, Z, ε, radial, axial, and azimuthal coordinates; ρ, density; V, velocity vector; P, pressure, W, azimuthal velocity; $\mathbf{r}$, unit radius vector; μ, effective viscosity; t, time; Y_k, mass fraction of components of mixture; I, internal energy; J, diffusion heat flux; λ, thermal conductivity; D, interdiffusion coefficient; Pr, Prandtl number; Sc, Schmidt number; h_k, chemical enthalpy of k-th component of mixture per unit volume; R_1, gas constant; T, temperature, °K; ω_k, molecular weight of k-th component; C_{vk}, specific heat of k-th component; ν, kinetic viscosity; ε, energy dissipation; μ_T, turbulent viscosity; μ_L, laminar viscosity; α, crack angle.

LITERATURE CITED

1. F. V. Bracco and P. J. O'Rourke, Prog. Energy Combust. Sci., 7 103-124 (1981).
2. T. D. Butler, L. D. Cloutman, J. K. Dukowicz, and J. D. Ramshaw, Prog. Energy Combust. Sci., 7, 293-315 (1981).
3. J. B. Heywood, in: Combustion Modeling in Reciprocating Engines, J. N. Mattavi and C. A. Aman (eds,), New York (1980), pp. 1-35.
4. F. V. Bracco, Introducing a New Generation of More Informative Combustion Models, SAE Paper 74174 (1974).
5. P. N. Blumberg, G. A. Lavoie, and R. J. Tabaczynski, Prog. Energy Combust. Sci., 5, 123-167 (1979).
6. H. Hiraki and J. M. Rife, Performance and NO_x Model of a Direct Injection of Stratified Charge Engine, SAE Tech. Pap. Ser. No. 800050 (1980).
7. H. B. Mathur, M. K. Gajendra Babu, and K. Subba Reddi, A Thermodynamic Simulation Model for a Methanol Fueled Spark Ignition Engine, SAE Tech. Pap. Ser. No. 830333 (1983).
8. R. E. Milane, R. J. Tabaczynski, and V. S. Arpaci, Combust. Sci. Technol., 32, 211-236 (1983).
9. A. A. Boni and G. P. Schneyer, One-Dimensional Area Computer Simulation of Combustion in a Divided Chamber Stratified Charge Engine, ASME Paper 75-WA/DGP-1 (1975).
10. S. C. Sorenson and S. S. Pan, A One-Dimensional Combustion Model for a Dual Chamber Stratified Charge Spark Ignition Engine, SAE Paper 790355 (1979).
11. L. C. Haselman, TDC – a Computer Code for Calculation of Chemically Reacting Hydrodynamic Flows in Two Dimensions, Lawrence Livermore Laboratory Report UCRL-52991 (May, 1980).
12. T. I.-P. Shih, G. E. Smith, G. S. Springer, and Y. Rimon, J. Comput. Phys., 52, 54-79 (1983).
13. J. J. Ramos, J. A. C. Humphrey, and W. A. Sirignano, Numerical Prediction of Axisymmetric Laminar and Turbulent Flows in Motored, Reciprocating Internal Combustion Engines, SAE Paper 790356 (1979).
14. L. D. Cloutman, J. R. Dukowicz, and J. D. Ramshaw, in: Proc. Seventh Int. Conf. Numerical Methods in Fluid Dynamics, Berlin (1981), pp. 119-124.
15. O. N. Lebedev and O. P. Solonenko, Izv. Sib. Otd. Akad. Nauk SSSR, Ser. Tekh. Nauk, No. 3, 117-125 (1980).
16. A. D. Gosman, R. J. R. Johns, W. Tipler, and A. P. Watkins, in: Proc. Thirteenth Int. Congr. Combustion Engines, Vienna (1979). CIMAC Session A4. D21.
17. Yu. M. Davydov, M. G. Kruglov, A. A. Mednov, and V. A. Nefedov, Numerical Study of Flows in Internal Combustion Engines by the Particle-in-Cell Method [in Russian], Moscow (1983).
18. Yu. M. Davydov, M. G. Kruglov, A. A. Mednov, and V. A. Nefedov, in: Aerophysics and Geocosmic Research [in Russian], Moscow (1983), pp. 40-44.

19. Yu. M. Davydov, M. G. Kruglov, A. A. Mednov, and V. A. Nefedov, in: Mathematical Methods of Control and Information Processing [in Russian], Moscow (1982), pp. 48-53.
20. F. Gracco and F. V. Bracco, AIAA J., 21, No. 4, 601-607 (1983).
21. A. Basso, in: Proc. Fourth Task Leaders Conf., Sept. 6-8, 1982, Italy (1983), pp. 41-47.
22. L. De Luca, F. Gamba, et al., in: Proc. Thirty-Fifth Congr. Nazionale Associazione Termotecnica Italiana (AIT), Saint Vincent, Sept. 15-19, 1982, Vol. 2, Italy (1982), pp. 641-654.
23. H. J. Schock and D. I. Sosoka, Numerical Studies of the Formation and Destruction of Vortices in a Motored Four-Stroke Piston–Cylinder Configuration, AIAA Paper No. 497 (1983).
24. P. O. Witze, Sandia Rep. No. 81-8242, Livermore, CA (1981).
25. V. E. Alemasov et al., Thermodynamic and Thermophysical Properties of Combustion Products (Handbook) [in Russian], Vol. 4, Moscow (1973).
26. D. Kwak, W. C. Reynolds, and J. H. Ferziger, in: Report No. TF-5, Stanford Univ., Stanford, CA (1975), p. 189.
27. O. J. McMillan, J. H. Ferziger, and R. S. Rogallo, in: AIAA Paper 80-1339 (1980), pp. 1-10.
28. J. W. Deardorff, J. Fluid Mech., 41, 453-467 (1970).
29. J. W. Deardorff, J. Comput. Phys., 8, 120-133 (1971).
30. J. D. Ramshaw, Informal Report, Los Alamos Scientific Laboratory Report LA-7955-MS (August, 1986).
31. W. C. Rivard, T. D. Butler, and O. A. Farmer, in: Proc. Fourth Int. Conf. Numerical Methods in Fluid Dynamics, Springer-Verlag, New York (1975), pp. 334-340.
32. F. H. Harlow and A. A. Amsden, J. Comput. Phys., 8, 197-213 (1971).
33. C. W. Hirt, in: Numerical Methods in Fluid Mechanics [Russian translation], Moscow (1973), pp. 156-164.
34. B. J. Daly, in: Proc. Fourth Int. Conf. Numerical Methods in Fluid Dynamics, Springer-Verlag, New York (1975).
35. P. O. Witze, in: Stratified Charge Automotive Engines, Inst. Mech. Eng. Conf. Publ., London (1980), pp. 25-31.

SYNTHESIS OF THERMOSTATING DEVICES.

II. MATHEMATICAL MODELS

G. N. Dul'nev and P. A. Korenev

UDC 536.24

The article deals with the procedure of designing (synthesis) of thermostating devices from the position of the systems approach. It compares the possibilities of the mathematical models used with this approach.

In the final analysis the designing of a thermostat consists in the realization of such boundary conditions for the object of thermostating which make it possible to attain the required (specified) space–time temperature field of the object, to ensure the specified error of thermostating and the specified time for attaining the operating regime, to satisfy requirements concerning overall dimensions, power consumption, weight, etc.

From this information on the permissible state of the system (the thermostat and the object of thermostating) we have to find the unknown causal characteristics, i.e., the boundary conditions for the object. These boundary conditions then enable us to choose the design of the thermostat and its operating regime. Such a statement of the problem makes it necessary to solve the inverse problem of heat exchange in a technical system [1]. From among various methods of solving inverse problems we will deal with the method of multiple realization ("scanning") of mathematical models whose essence reduces to the following operations: a) on the basis of some considerations the prototype of the design (basic model)

Leningrad Institute of Precision Mechanics and Optics. Translated from Inzhenerno-Fizicheskii Zhurnal, Vol. 51, No. 4, pp. 660-667, October, 1986. Original article submitted June 10, 1985.

0022-0841/86/5104-1243$12.50